THEORY, ANALYSIS , DESIGN METHODOLOGY, RESISTANCE AND PROPULSION OF SHIPS

Yoshiaki Kodama
National Maritime Research Institute, Japan

Keywords: Actuator disk, Bernoulli's theorem, Biot-Savart's law, boundary layer, boundary layer equation, cavitation, cavitation number, CFD, circulation, continuity equation, Dirichlet condition, displacement thickness, divergence-free condition, doublet, eddy viscosity, elementary wave, finite-volume method, form factor, free surface, friction velocity, Froude's hypothesis, Froude number, group velocity, Hess and Smith panel method, hull efficiency, ideal efficiency, induced drag, induced velocity, ITTC'78 curve, Kelvin waves, kutta condition, Laplace equation, level set method, linearized free-surface boundary condition, MAC method, mach number, mass conservation, momentum conservation, momentum thickness, Navier-stokes equation, Neumann condition, Newtonian fluid, numerical stability, pitot tube, POT, potential flow, pseudo-compressibility method, Rankine-source method, RANS, relative rotative efficiency, resistance, Reynolds number, Reynolds stress, Schoenherr's flat plate friction line, singularity, source, Stokes' theorem, structured grid, Taylor wake, thrust deduction coefficient, torricelli's theorem, turbulence model, unstructured grid, upwinding, upwind differencing, VOF, vortex filament, vorticity, 1/7-th power law

Contents

Summary

Basic hydrodynamic phenomena that occur around ships and propellers are explained with a focus on the conservation properties of mass and momentum. Taking advantage of the characteristics of the flow, the potential flow approximation, which is valid to flows except for the vicinity of the solid wall where the boundary layer develops due to viscosity. In the potential flow, singularities characterize the flow.

The Navier-Stokes equations, the governing equations of the water flow, are derived from the conservation laws of mass and momentum.

The potential flow is derived by approximating the Navier-Stokes equations. The approximation is shown to be valid in many types of flows around a ship and a propeller. It is shown how the vorticity is generated in the boundary layer on a wing-like body by viscosity. Vorticity causes circulation and lift.

In the high Reynolds-number flow past a streamlined body such as a ship, a thin boundary layer develops along the body surface. The properties of the boundary layer are explained using the boundary-layer equations.

Propulsion of a ship is almost always carried out by a rotating screw propeller located at the stern. Propeller efficiency is explained using the momentum theory. A standard procedure for testing a model propeller is explained. Hull-propeller-rudder interactions are explained. Cavitation is explained as a boiling process at normal temperature.

Properties of free-surface waves generated by a ship advancing on the water are explained using the linearized free-surface boundary condition in the potential flow. It is shown that the 2D wave-making drag due to two wave sources has humps and hollows

by interference. The 3D wave pattern called Kelvin waves is derived.

An experimental method to estimate the drag of a full-scale ship based on the measured drag of a ship model is explained.

Lastly, CFD, i.e. numerical methods to solve the Navier-Stokes equations for incompressible flows, is explained. Grid topologies, how to derive a set of simultaneous equations of flow variables at discrete points, upwinding to compute high Reynolds number flows, turbulence modeling for the Reynolds stresses, how to treat free-surface waves, and how to use CFD as a user are explained.

1. Introduction

A ship advancing on the water surface experiences various kinds of hydrodynamic forces from the surrounding water. Perhaps the closest analogy is an airplane flying in the air. By closely looking at the similarities and differences between the two, one can understand the nature of the hydrodynamic phenomena around ships.

First, the water density. At $20C^\circ$ the density of air is $\rho_\mathrm{a} = 1.205\times 10^{-3}\ \mathrm{g/cm^3}$ while that of water is $\rho_\mathrm{w} = 0.998\mathrm{g/cm^3}$, 829 times that of air. This is why a ship runs much more slowly than an airplane, because, since the hydrodynamic force is proportional to the speed squared U^2, to get the same magnitude of hydrodynamic force, a ship should run at speed 1/29 of an airplane. Actually, a typical cruising speed of a Jumbo Jet is 913km/hr, whose 1/29 is 31km/hr, while that of a large tanker of length exceeding 300m is 14 ~ 16 knots (26 ~ 30 km/hr).

Air and water are among the least viscous fluids. The viscosity of air is $\mu_\mathrm{a} = 18.2\times 10^{-3}\mathrm{N.sec/m^2}$, while that of water is even smaller, being $\mu_\mathrm{a} = 1.002\times 10^{-3}\mathrm{N.sec/m^2}$, both at $20C^\circ$. This is why we, including fish, can move rather freely in air or water.

Although very small, viscosity plays a crucial role in the immediate vicinity of the hull surface, causing macroscopic forces such as frictional drag and lift. Propeller thrust cannot be generated without viscosity.

Throughout the chapter the fluid, i.e. water, is assumed incompressible. A fluid can be regarded as incompressible so long as the Mach number M, the ratio of the flow speed U to the speed of sound c, is small.

$$M = \frac{U}{c} << 1 \qquad (1)$$

In case of sea water at 20 degree Celsius, $c = 1513\mathrm{m/s}$, and therefore the assumption of incompressibility almost always holds. In contrast, air is compressible. In compressible flows, energy conservation must be taken into account, in addition to mass and momentum conservations taken into account in incompressible flows as well. Also, incompressible flow solvers have clear distinction from compressible flow solvers in CFD.

Water has one the largest latent heat values among existing fluids. This is why our planet Earth, whose vast amount of water stabilizes temperature, can accommodate life. This property renders heat transfer a passive role in hydrodynamics.

The flow around a ship is an external flow, where a solid body is surrounded by the flow domain of nearly infinite size. To this type of flows, the potential flow, described in Section 3, is a useful approximation. This situation is in contrast to internal flows frequently met in mechanical engineering, where the flow domain is bordered by a solid wall, like the flow in a duct, and the viscous force is non-negligible almost everywhere.

Free-surface waves generated by a ship advancing on the water characterize ship hydrodynamics. Potential flow is a useful approximation to handle free-surface waves. In this chapter, only the simplest cases of free-surface waves including wave-making drag are explained within the context of potential flow with linearized free-surface boundary conditions. Although very important, neither ship motion in waves nor the added mass effect is explained in this chapter.

The refs. [Newman (1977), Lewis (1988), Schlichting (1999), Ferziger and Peric (2002), Suzuki (2006)] have been particularly useful in compiling this chapter. omprehensive research activities by the ITTC (International Towing Tank Conference), consisting of specialists in ship hydrodynamics, can be found in ref. [ITTC web site].

2. Conservation Laws

Fluid motion is governed by a set of conservation laws. A conservation law states that the net flux of a physical property across the surface bounding a control volume is zero, if there are no sources or sinks inside. An equation for a conservation law is obtained by setting up a cubic control volume in space, summing up all the fluxes that go in and out of the control volume, and equating it with zero.

2.1. Mass Conservation

As shown in Figure 1, where $[u \quad v \quad w]^{\mathrm{T}}$ are the velocity components in *x*-, *y*-, and *z*-directions, the mass flux across the surface of the area $\Delta y \Delta z$, whose normal vector is in the positive *x*-direction, is $\rho u \Delta y \Delta z$. Setting the out-flux as positive, the summation of the mass flux across the two surfaces in the *x*-direction, Δx apart from each other, results in $-\rho \frac{\partial u}{\partial x} \Delta x \Delta y \Delta z$, and similarly $-\rho \frac{\partial v}{\partial y} \Delta x \Delta y \Delta z$ and $-\rho \frac{\partial w}{\partial z} \Delta x \Delta y \Delta z$ in *y*- and *z*-directions. Thus the mass conservation, which sets the total mass flux as zero, results in

$$-\rho\left(\frac{\partial u}{\partial x}+\frac{\partial v}{\partial y}+\frac{\partial w}{\partial z}\right)\Delta x\Delta y\Delta z=0$$

$$\downarrow$$

$$\frac{\partial u}{\partial x}+\frac{\partial v}{\partial y}+\frac{\partial w}{\partial z}=0 \quad \text{or } \vec{\nabla}\cdot\vec{u}=0 \quad \text{or } \operatorname{div}\vec{u}=0 \tag{2}$$

where $\vec{\nabla}=\begin{bmatrix}\partial/\partial x\\ \partial/\partial y\\ \partial/\partial z\end{bmatrix}$ is the gradient operator, and "*div*" is divergence. The Eq.(2) is called the continuity equation or the divergence-free condition.

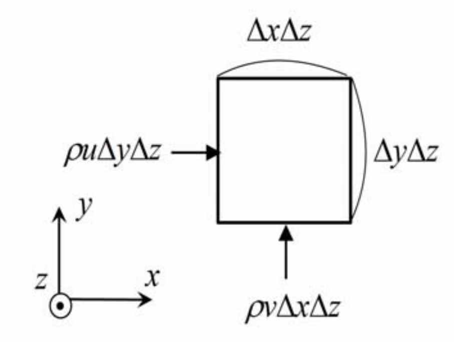

Figure 1. Mass flux

2.2. Momentum Conservations

<u>*x*-momentum</u>

The *x*-momentum flux is generated not only by the mass flux but also by the stress tensor consisting of pressure and viscous stresses.

Again setting the in-flux as positive, the net mass flux across the two surfaces in the *x*-direction, Δx apart, generates the *x*-momentum flux $-\rho\frac{\partial(u^2)}{\partial x}\Delta x\Delta y\Delta z=-2\rho u\frac{\partial u}{\partial x}\Delta x\Delta y\Delta z$. Similarly, the net mass flux across the two surfaces in the *y*-direction generates $-\rho\frac{\partial(uv)}{\partial y}\Delta x\Delta y\Delta z=-\rho\left(v\frac{\partial u}{\partial y}+u\frac{\partial v}{\partial y}\right)\Delta x\Delta y\Delta z$, and $-\rho\frac{\partial(uw)}{\partial z}\Delta x\Delta y\Delta z=-\rho\left(w\frac{\partial u}{\partial z}+u\frac{\partial w}{\partial z}\right)\Delta x\Delta y\Delta z$ in *z*-direction. Summing the three components and using the divergence-free condition results in

$$-\rho\left(u\frac{\partial u}{\partial y}+v\frac{\partial u}{\partial y}+w\frac{\partial u}{\partial y}\right)\Delta x\Delta y\Delta z \tag{3}$$

The contribution of pressure and viscous stress to the *x*-momentum flux is expressed by a stress tensor P. In the water flow, assuming that it is incompressible, that it is

Newtonian fluid (i.e. the stress is proportional to the rate of strain), and that the Stokes relation holds, the stress tensor P is expressed by

$$P = p_{ij} = -p\delta_{ij} + \mu e_{ij} = -p\delta_{ij} + \mu\left(\frac{\partial u_i}{\partial x_j} + \frac{\partial u_j}{\partial x_i}\right) = \begin{bmatrix} -p + 2\mu\frac{\partial u}{\partial x} & \mu(\frac{\partial u}{\partial y} + \frac{\partial v}{\partial x}) & \mu(\frac{\partial u}{\partial z} + \frac{\partial w}{\partial x}) \\ \mu(\frac{\partial v}{\partial x} + \frac{\partial u}{\partial y}) & -p + 2\mu\frac{\partial v}{\partial y} & \mu(\frac{\partial v}{\partial z} + \frac{\partial w}{\partial y}) \\ \mu(\frac{\partial w}{\partial x} + \frac{\partial u}{\partial z}) & \mu(\frac{\partial w}{\partial y} + \frac{\partial v}{\partial z}) & -p + 2\mu\frac{\partial w}{\partial z} \end{bmatrix} \tag{4}$$

where p is pressure, δ_{ij} is Kronecker's delta, and μ is the molecular viscosity. Then the force acting on the surface with a unit normal vector $\vec{n}$ is $P\vec{n}$. On the surface facing the positive *x*-direction, where $\vec{n} = \begin{bmatrix} 1 \\ 0 \\ 0 \end{bmatrix}$, the force acting in the *x*-direction is $[-p + \mu(2\frac{\partial u}{\partial x})]\Delta y \Delta z$. Thus the summation of the *x*-direction forces acting on the surfaces facing positive and negative *x*-directions, Δx apart, results in $[-\frac{\partial p}{\partial x} + \mu(2\frac{\partial^2 u}{\partial x^2})]\Delta x \Delta y \Delta z$. On the surface facing the positive *y*-direction where $\vec{n} = \begin{bmatrix} 0 \\ 1 \\ 0 \end{bmatrix}$, the force acting in the *x*-direction is $[\mu(\frac{\partial u}{\partial y} + \frac{\partial v}{\partial x})]\Delta x \Delta z$. Thus the summation of the *x*-direction forces acting on the surfaces facing positive and negative *y*-directions, Δy apart, results in $[\mu(\frac{\partial^2 u}{\partial y^2} + \frac{\partial^2 v}{\partial x \partial y})]\Delta x \Delta y \Delta z$. Similarly, the summation of the *x*-direction forces acting on the surfaces facing positive and negative *z*-directions, Δz apart, results in $[\mu(\frac{\partial^2 u}{\partial z^2} + \frac{\partial^2 w}{\partial x \partial z})]\Delta x \Delta y \Delta z$. Summing the three components and using the divergence-free condition results in

$$\left[-\frac{\partial p}{\partial x} + \mu\left(\frac{\partial^2 u}{\partial x^2} + \frac{\partial^2 u}{\partial y^2} + \frac{\partial^2 u}{\partial z^2}\right)\right]\Delta x \Delta y \Delta z \tag{5}$$

Summation of Eqs.(3) and (5) is equated to the *x*-momentum change inside the control volume per unit time, thus

$$\rho\frac{\partial u}{\partial t}\Delta x \Delta y \Delta z = -\rho\left(u\frac{\partial u}{\partial y} + v\frac{\partial u}{\partial y} + w\frac{\partial u}{\partial y}\right)\Delta x \Delta y \Delta z + [-\frac{\partial p}{\partial x} + \mu(\frac{\partial^2 u}{\partial x^2} + \frac{\partial^2 u}{\partial y^2} + \frac{\partial^2 u}{\partial z^2})]\Delta x \Delta y \Delta z$$

$$\downarrow$$

$$\frac{\partial u}{\partial t}+u\frac{\partial u}{\partial x}+v\frac{\partial u}{\partial y}+w\frac{\partial u}{\partial z}=-\frac{1}{\rho}\frac{\partial p}{\partial x}+\nu(\frac{\partial^2 u}{\partial x^2}+\frac{\partial^2 u}{\partial y^2}+\frac{\partial^2 u}{\partial z^2}) \tag{6}$$

where

$\nu \equiv \dfrac{\mu}{\rho}$: kinematic viscosity

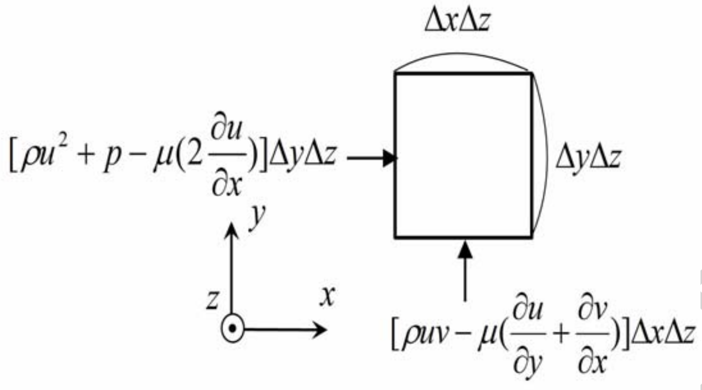

Figure 2. *x*-momentum flux

Similarly the *y*-momentum and *z*-momentum equations are
y-momentum

$$\frac{\partial v}{\partial t}+u\frac{\partial v}{\partial x}+v\frac{\partial v}{\partial y}+w\frac{\partial v}{\partial z}=-\frac{1}{\rho}\frac{\partial p}{\partial y}+\nu(\frac{\partial^2 v}{\partial x^2}+\frac{\partial^2 v}{\partial y^2}+\frac{\partial^2 v}{\partial z^2}) \tag{7}$$

z-momentum

$$\frac{\partial w}{\partial t}+u\frac{\partial w}{\partial x}+v\frac{\partial w}{\partial y}+w\frac{\partial w}{\partial z}=-\frac{1}{\rho}\frac{\partial p}{\partial z}+\nu(\frac{\partial^2 w}{\partial x^2}+\frac{\partial^2 w}{\partial y^2}+\frac{\partial^2 w}{\partial z^2}) \tag{8}$$

Generally, there are cases in which an external force $\vec{K}$, also called body force, acts on the fluid per unit mass. Then the momentum equations are, in vector form,

$$\frac{\partial \vec{u}}{\partial t}+(\vec{u}\cdot\vec{\nabla})\vec{u}=\vec{K}-\frac{1}{\rho}\vec{\nabla}p+\nu\Delta\vec{u} \tag{9}$$

where

Laplacian operator $\Delta \equiv (\vec{\nabla}\cdot\vec{\nabla}) = \dfrac{\partial^2}{\partial x^2}+\dfrac{\partial^2}{\partial y^2}+\dfrac{\partial^2}{\partial z^2}$ (10)

For example, if there is gravity, $\vec{K}=\vec{K}_{\rm g}\equiv\begin{bmatrix}0\\0\\-g\end{bmatrix}$, where g =9.8m/s^2, the acceleration of gravity.

Conservation laws can be more easily handled if they are non-dimensionalized using a representative length L and a speed U. In case of a running ship, L should be the ship length and U be the ship speed. Defining non-dimensional variables $\vec{u}^*\equiv\frac{\vec{u}}{U}$, $x^*\equiv\frac{x}{L}$, $t^*\equiv\frac{t}{L/U}$, $p^*\equiv\frac{p}{\rho U^2}$, and omitting * for simplicity, Eq.(9) with $\vec{K}=\vec{K}_{\rm g}$ becomes

$$\frac{\partial\vec{u}}{\partial t}+(\vec{u}\cdot\vec{\nabla})\vec{u}=\vec{K}_{\rm g}-\vec{\nabla}p+\frac{1}{R_{\rm e}}\Delta\vec{u} \quad (11)$$

where

$$\vec{K}_{\rm g}\equiv\begin{bmatrix}0\\0\\-\frac{1}{F_r^2}\end{bmatrix},\ R_{\rm e}\equiv\frac{UL}{\nu}:\text{Reynolds number},\quad F_{\rm r}\equiv\frac{U}{\sqrt{gL}}:\text{Froude number.} \quad (12)$$

Eq.(11) is called the Navier-Stokes equations. Another form of the NS equation is

$$\frac{\partial u_i}{\partial t}+\frac{\partial}{\partial x_j}\left[u_iu_j+p\delta_{ij}-\frac{1}{R_{\rm e}}\left(\frac{\partial u_i}{\partial x_j}+\frac{\partial u_i}{\partial x_j}\right)+\frac{1}{F_{\rm r}^2}x_3\right]=0,\quad (i=1,2,3) \quad (13)$$

The Reynolds number $R_{\rm e}$ expresses the ratio of inertia force to viscous force.

$$\frac{[\text{inertia force}]}{[\text{viscous force}]}=\frac{\rho u^2}{\mu\frac{\partial u}{\partial y}}\approx\frac{\rho U^2}{\mu\frac{U}{L}}=\frac{UL}{\frac{\mu}{\rho}}=\frac{UL}{\nu} \quad (14)$$

Since the kinematic viscosity of water is very small, the Reynolds number is very large. With a full-scale ship it is $O[10^9]$, and $O[10^7]$ with a ship model of a few meters in length. Therefore flows around ships are high Reynolds-number flows.

In compressible flows, energy conservation must be taken into account, in addition to mass and momentum conservations.

-
-
-

Bibliography

CFD Workshop Tokyo (2005). Test Case 1.1, Figure 1.1-5. http://www.nmri.go.jp/cfd/cfdws05/

Chorin, A.J. (1967). A Numerical Method for Solving Incompressible Viscous Flow, *Journal of Computational Physics*, vol. 2. pp.12-26.

Dawson, C.W. (1977). A Practical Computer Methods for Solving Wave Program, Proc. 2nd International Conference on Numerical Ship Hydrodynamics, Berkeley, pp.30-38.

Ferziger, J.H., Peric, M. (2002). *Computational Methods for Fluid Dynamics*, 3rd Edition, Springer.

Harlow, F.H., Welch, J.E. (1965). Numerical Calculation of Time-Dependent Viscous Incompressible Flow of Fluid with Free Surface, *Physics of Fluids*, vol.8, pp.2182-2189.

Hess, J., Smith, A.M.O. (1994). Calculation of nonlifting potential flow about arbitrary three-dimensional bodies. *J. Ship Research*, 8, pp. 22-44.

Hino, T. (1998). Navier-Stokes Computations of Ship Flows on Unstructured Grids, Proceedings of the 22nd Symposium on Naval Hydrodynamics, Washington.

Hirata, N., Hino, T. (1999). A Comparative Study of Zero- and One-Equation Turbulence Models for Ship Flows with/without Free Surface, Proceedings of the Kansai Society of Naval Architecture.

Hirt, C.W., Nicholls, B.D. (1981). Volume of Fluid (VOF) methods for dynamics of free boundaries, *J. of Computational Physics*, vol.39, pp.201-221.

ITTC web site. (http://ittc.sname.org/).

Kodama, Y. (1992). Computation of Ship's Resistance Using an NS Solver with Global Conservation, *J. of the Society of Naval Architects of Japan*, Vol.172, pp.147-155.

Launder B.E., Spalding D.B. (1972). *Lectures in Mathematical Models of Turbulence*. Academic Press, London, England.

Lewis, E.V. (1988). *Principles of Naval Architecture Vol. II - Resistance, Propulsion and Vibration*, SNAME.

Menter, F.R. (1994). Two-Equation Eddy-Viscosity Turbulence Models for Engineering Applications, *AIAA Journal*, vol.32, No.8, pp.1598-1605.

Nakashima Propeller web site. (http://www.nakashima.co.jp/tech/tech3.html).

Newman, J.N. (1977). *Marine Hydrodynamics*, MIT.

PBCF web site. (http://pbcf.motech.co.jp/english/index.html).

Schlichting, H. (1999). *Boundary-Layer Theory*, Springer.

Sethian, J.A., Smereka, P. (2003). Level Set Methods for Fluid Interfaces, *Annual Review of Fluid Mechanics*, volume 35, pp.341-372.

Sussman, Smereka, Osher (1994), A Level Set Approach for Computing Solutions to Incompressible Two-Phase Flow, *J. of Computational Physics* vol.114(1), pp.146-159.

Suzuki, K. (2006). Theory of Fluid Dynamics and Fluid Dynamic Drag (in Japanese), Seizando.

Wikipedia: *Propeller* (http://en.wikipedia.org/wiki/Propeller)

Biographical Sketch

Dr. Yoshiaki Kodama has been engaged in research on ship hydrodynamics. He studied cavitation inception using simple test bodies. He developed a CFD code for ship flows using the pseudo-compressibility method. Recently he carried out drag reduction studies using air lubrication. He served as the Editor-in-Chief of the Journal of Marine Science and Technology (2006-2009).